ORIGINAL PAPER

CrossMark

Chitosan Functionalization with Amino Acids Yields to Higher Copper Ions Adsorption Capacity

Cynthia R. A. Mahl[1] · Thiago B. Taketa[1] · Rogério A. Bataglioli[1] · Eduardo José de Arruda[2] · Marisa M. Beppu[1]

Abstract

Chitosan (Chi) beads were conjugated with three different amino acids [namely, glutamic acid (GLU), methionine (MET), and taurine (TAU)] aiming to increase the divalent copper ions uptake in aqueous media. Scanning Electron Microscopy evidenced the development of a large porous structure after amino acid functionalization, associated with the increase in a number of amino groups in the polymer backbone. X-Ray Photoelectron Spectroscopy and Fourier-Transform Infrared Spectra analyses were also employed to assess the conjugation of these three different amino acids in chitosan backbone. Adsorption experiments were conducted in a batch process, at 298 K, and kinetic data indicated a slightly better fitting for the pseudo-first-order model when compared to pseudo-second order. Intraparticle diffusion model suggested a three-step mechanism for Cu(II) adsorption kinetics, limited by the third step, the intraparticle diffusion. The isotherm data fitting to the traditional Langmuir and Freundlich models indicated a better fit for the former case. The amino acid conjugation resulted in the increase of the maximum adsorption capacity for Cu(II) from 1.30 mmol g^{-1} prior to amino acid conjugation to values as high as 2.31 mmol g^{-1}, 2.40 mmol g^{-1} and 2.68 mmol g^{-1} for Chi–TAU, Chi–GLU, and Chi–MET, respectively. These results are attributed to the introduction of additional amino groups and new carboxylate and amino acid residues into the chitosan backbone, which might also be explored for amino acid demanding applications.

Cynthia R. A. Mahl, Thiago B. Taketa, and Rogério A. Bataglioli have equally contributed to this work.

Electronic supplementary material The online version of this article (https://doi.org/10.1007/s10924-018-1306-4) contains supplementary material, which is available to authorized users.

✉ Thiago B. Taketa
thiagobt@gmail.com

Cynthia R. A. Mahl
cramahleq@gmail.com

Rogério A. Bataglioli
rogerbataglioli@gmail.com

Eduardo José de Arruda
eduardoarruda@ufgd.edu.br

Marisa M. Beppu
beppu@feq.unicamp.br

[1] Faculdade de Engenharia Química, Universidade Estadual de Campinas, Av. Albert Einstein 500, Campinas, SP CEP 13083-852, Brazil

[2] Universidade Federal da Grande Dourados, Rodovia Dourados - Itahum, Km 12, Dourados, MS CEP 79804-970, Brazil

Introduction

Heavy metal contamination on aquatic effluents presents one of the most severe threats to the environment due to their recalcitrant and highly toxic effects to organisms [1, 2]. Copper, for example, one the most abundant metals employed in the industry, has an essential metabolic function; however, when ingested in excess (over 1.3 mg L^{-1}) [3], copper may cause symptoms ranging from vomit and convulsion to death. This scenario challenges the scientific community to look up for more efficient, low-cost alternatives for the removal of heavy metal species from aquatic media, in concentrated and diluted conditions.

Different strategies have been explored for the removal of heavy metal species from wastewater such as chemical precipitation [4], membrane filtration [5], electrochemical treatment [6], flocculation and coagulation [7], and adsorption [8, 9]. Because of its effectiveness and flexibility to use low-cost or inexpensive non-living materials as sorbents [10, 11], adsorption is recognized as one of the most convenient processes for heavy metal wastewater treatment, especially

in developing countries [1]. As a drawback, these low-cost sorbents may present complications for heavy metal desorption, which requires new strategies for their separation from the heavy metals for proper disposal [1].

Chitosan, the deacetylated form of the most abundant chitin [12], is a linear copolymer composed of β-(1→4) D-glucosamine and *N*-acetyl-D-glucosamine units, widely explored for removing heavy metals from aqueous media [13, 14]. Similar to most biopolymers, chitosan uptakes cationic heavy metal species by ionic exchange through chelation, using the specific three-dimensional arrangements of its amino and hydroxyl groups to capture ions of a specific size into the matrix [15]. Anionic species are easily taken from the aqueous media by electrostatic attraction with the protonated amino groups of chitosan under acidic conditions [16]. The amino radicals in the C-2 position of the glucosamine monomer also yield to chitosan solubility under acidic conditions [12], allowing the production of chitosan-based materials into various shapes such as membranes [17, 18], beads [19], thin films [20] and microparticles [21].

Different chemical treatments have been studied to improve both the mechanical stability and metal ion adsorption capacity of chitosan-based materials. Bifunctional crosslinking agents such as glutaraldehyde and epichlorohydrin are employed to assure the stability of chitosan under acidic condition [8, 22]. Nevertheless, these functionalization reactions might reduce the heavy metal adsorption capacity, depending on the crosslinking agent employed and the extent of the reaction [8].

Immobilization of polyfunctional species [23], such as ethylenediaminetetraacetic acid (EDTA) [24], with high affinity to specific metal species, has been reported as a method to improve the adsorption and the binding selectivity of chitosan adsorbents. Recently, conjugation of amino acid moieties with chitosan has emerged as an alternative for increasing the adsorption capacity of chitosan-based materials [25], by introducing carboxylate, amino groups, and the additional amino acid residues functionalities into the polymer backbone. Beppu et al. [49] reported the increase of the maximum adsorption capacity for Cu(II) of high porous chitosan membrane after histidine immobilization, which might be attributed to the Cu(II) binding to the amino and imidazole functionalities of the amino acid moieties. Boggione et al. [19] also investigated chitosan membranes functionalized with both amino acids (namely, L-aspartic acid, L-glutamic acid, L-histidine, and L-taurine) and Cu(II) to improve the selective adsorption of the endoglucanase, illustrating the use of chitosan membranes after heavy metal uptake for biotechnological purposes. Despite these promising examples, to our knowledge, there is a lack of studies that explore both the equilibrium and kinetic adsorption behavior of chitosan-based materials after amino acid conjugation.

The present study investigates the adsorption of Cu(II) onto chitosan beads conjugated with three different amino acids (namely glutamic acid, methionine, and taurine). Equilibrium adsorption data were fitted to the traditional Langmuir and Freundlich models, and the kinetic data were modeled by three different equations to investigate the mechanism governing this phenomenon. Morphological changes in chitosan beads were monitored by Scanning Electron Microscopy (SEM), and their chemical changes were assessed by X-Ray Photoelectron Spectroscopy (XPS) and Fourier-Transformed Infrared Spectroscopy (FTIR-ATR) techniques. Functionalized chitosan beads present higher, although less energetically favorable, copper ion adsorption capacities, which suggests their use for heavy metal adsorption or for those processes in which specific amino acid interaction are required.

Experimental

Materials

Chitosan of commercial degree with a minimum of 75% deacetylation, and the amino acids L-glutamic acid (GLU), taurine (TAU) and L-methionine (MET) were provided by Sigma-Aldrich, USA. Copper nitrate used in adsorption experiments was provided by Merck, Germany. Epichlorohydrin (EPI), acetic acid, and sodium hydroxide were purchased by Synth, Brazil. All reagents were analytical grade.

Preparation of Chitosan Beads

Chitosan was dissolved in aqueous acetic acid 3% (v/v) solution with mechanical agitation for 72 h, producing a final solution with 2.5% (w/w) biopolymer. Chitosan beads were prepared by dropping this solution into a 1.0 mol L^{-1} aqueous solution of NaOH bath, under regular stirring, and kept immersed for 24 h. These beads were extensively washed with distilled water until all alkali was removed and stored in ultrapure water at 4 °C.

Functionalization of Chitosan Beads with Amino Acids

The functionalization of chitosan beads with amino acids was carried out using the method suggested by Sano and Murase [26]. Firstly, EPI and the amino acid were mixed in an equimolar proportion by adding 0.78 mL EPI solution to a bath solution of NaOH (2 mol L^{-1}) containing 1.47 g of GLU, 1.25 g of TAU or 1.49 g of MET. The remaining solution was mixed for 4 h at 60 °C and immediately cooled down to 0 °C, followed by the addition of 22 g of NaOH under constant stirring. Wet chitosan beads (20 g)

were added to this solution, and the functionalization was conducted at 65 °C for 16 h under constant stirring. After the reaction, beads were extensively washed with distilled water until reaching neutral pH and stored in ultrapure water at 4 °C [27]. Supplementary Information (Fig. S1) shows the reactions involved in this functionalization, according to the mechanisms proposed by Adhikari et al. [27].

Adsorption Experiments

Adsorption experiments were carried out in $Cu(NO_3)_2$ aqueous solution at pH 5.0, under constant stirring at 150 rpm at 25 °C. Equilibrium adsorption tests were performed using the static method: 25 mL of copper solution with concentrations ranging from 0.08 to 12 mol L^{-1} were placed in plastic flasks containing 0.3 g of natural or amino acid functionalized chitosan beads. The beads were kept in solution under agitation until the equilibrium was reached, i.e., when copper concentration did not change over time. The concentration of Cu(II) in solution was determined by an atomic absorption spectrometer (Perkin Elmer AA Analyst 100 flame oxidizing air-acetylene). Adsorption capacity, Q, was calculated using the Eq. 1:

$$Q = (C_0 - C_e)\frac{V}{m} \tag{1}$$

where C_0 is the initial concentration of Cu(II) and C_e is final concentration of Cu(II), both in (mmol L^{-1}), V is the volume (L) and, m is the wet mass of chitosan beads (g):

For batch kinetic experiments, 4.8 g of wet chitosan beads were soaked in 1 L of 0.47 mol L^{-1} Cu(II) solution over 48 h, withdrawing 1.0 mL aliquots of the solution at fixed time intervals for measuring Cu(II) concentration. Aliquot volumes were kept minimal to reduce experiment disturbances, and their influence in the overall solution volume was taken into account when calculating Cu(II) concentration.

Characterization of the Adsorbent

Scanning Electron Microscopy (SEM)

Morphological changes in chitosan beads with amino acids functionalization and copper adsorption were assessed by SEM. Prior to analysis, samples were frozen in liquid nitrogen and lyophilized to remove the water from their pores. Shortly after, samples were sputter coated with a thin layer of gold and probed in an LEO-440i (Cambridge Instruments, England) scanning electron microscope at 10.00 kV and 50 pA, using a magnification of ×1000.

Fourier-Transform Infrared Spectroscopy with Attenuated Total Reflectance (FTIR-ATR)

Amino acid functionalization and copper uptake in the surface of chitosan beads were chemically followed with FTIR-ATR analyses, carried out in Thermo Nicolet 6700 equipment (Thermo Fisher Scientific, USA), with ATR accessory Smart Omni-Sampler. All spectra were obtained in a range of 4000–650 cm^{-1}, with a resolution of 4 cm^{-1}.

Deacetylation Degree (DD)

The relative amount of amino groups in chitosan chain also referred as chitosan DD, may be determined by simple pH-potentiometric titration analysis. In this method, 0.3 g of natural or functionalized chitosan beads were dried at 60 °C until reaching a constant weight and dissolved in 25 mL of standard HCl solution (0.02 mol L^{-1}), in excess, for 24 h to protonate the available amino groups. The resulting solution was titrated with NaOH solution (0.1 mol L^{-1}), in standard atmosphere condition, and the DD of chitosan and chitosan functionalized beads were calculated according to Eq. 2:

$$DD(\%) = \frac{C_{NaOH} \times (V_2 - V_1) \times 161}{m_2} \times 100 \tag{2}$$

in which C_{NaOH} (mol L^{-1}) is the concentration of the NaOH titrant solution; V_1 and V_2 (L) are, respectively, the volume of NaOH used for neutralizing the excess of HCl and the chitosan protonated groups; 161 (g mol^{-1}) is the molecular weight of chitosan monomer unit; and m_2 (g) is the weight of dry sample used for titration.

Three replicates were performed for each sample. These procedure results in the titration curve with two inflection points: while the first point corresponds to the excess of HCl, the second one is related to the protonated sites of chitosan.

X-Ray Photoelectron Spectroscopy (XPS)

XPS analyses of Chi, Chi–MET, Chi–GLU and Chi–TAU were carried out on a Physical Electronics Versaprobe II X-ray Photoelectron Spectrometer with a monochromated Al source (1486.6 eV; 50 W; spot size of 200 μm) to verify the surface modifications of chitosan beads due to the functionalization with amino acids and the adsorption process as well. Data were treated using Casa XPS software, and the relative sensitivity factors for the elements were provided by PHI's MultiPak processing software. Binding energies were charged-corrected to 285.0 eV for the carbon–carbon bond, and the spectra were smoothed using a seven-point quadratic Savitzky–Golay method. The XPS spectra peaks were decomposed into sub-components by fixing the 20% Lorentzian–Gaussian curve-fitting program with a Shirley

background. For the high-resolution (HR) spectra, the passing energy employed was 23.5 eV with a binding energy range of 278–298 eV for C1s (two sweeps) and 391–401 eV for N1s (six sweeps).

Results and Discussion

Copper Speciation

Solution pH was set 5.0, taking into account copper speciation analysis performed in HYDRA® (Hydrochemical Equilibrium-Constant Database) software. According to the speciation diagram of copper nitrate (Fig. S2), at pH values lower than 5, copper is found in solution as Cu(II). In that condition, the adsorption capacity of chitosan beads decreases due to protonation of amino groups, which induces the electrostatic repulsion of Cu(II) cations, and metal adsorption mainly occurs by chelation with hydroxyl and amino groups of chitosan [8]. Also, at pH values higher than 6, Cu(II) precipitates in hydroxide form. Facing this scenario, we decided to run our experiments at pH 5. Other authors conducted adsorption experiments by changing the initial pH and evaluating the adsorption capacity, and they verified the same pH value as an optimum for adsorption of copper ions in chitosan beads [28–30].

Copper Adsorption

Equilibrium adsorption results were adjusted to both Langmuir, and Freundlich adsorption models for a more accurate comparison of the adsorption behavior among amino acid functionalized chitosan beads. The Langmuir model (Eq. 3), which is the simplest adsorption model available, assumes the molecules are adsorbed in the surface in a monolayer fashion, the adsorption sites are energetically equivalent, and there is no interaction between adjacent adsorbed molecules [31].

$$Q_e = \frac{bQ_{max}C_e}{1 + bC_e} \tag{3}$$

In Eq. 3, C_e represents the equilibrium concentration of Cu(II) in solution (mmol L^{-1}); Q_e is the uptake capacity of Cu(II) at equilibrium concentration (mmol g^{-1}), Q_{max} is the maximum adsorption capacity of adsorbent (mmol g^{-1}) and b is the Langmuir binding constant, which is related to the energy of adsorption (L $mmol^{-1}$).

The Freundlich isotherm (Eq. 4) is an empirical model generally used to describe the adsorption in a heterogeneous surface, which also assumes an exponential distribution of active sites and energies in the surface [32].

$$Q_e = K_F C_e^{1/n} \tag{4}$$

here K_F is the Freundlich constant related to the adsorption capacity and n is the heterogeneity factor related to adsorption intensity.

Experimental data for natural and amino acid functionalized chitosan beads are presented in Fig. 1, with the respective fit for both Langmuir and Freundlich isotherms. The parameters for each model were calculated by Origin® software, based on the nonlinear method, and Table 1 lists the parameters obtained and their respective correlation coefficients (R^2), employed for checking the quality of data-fitting. Figures S3 and S4 show the normal probability plot of regular residuals for Langmuir and Freundlich models, respectively. Points very close to the line and p value > 0.05 indicate the normal distribution of the data (according to the Anderson–Darling test for normality) for all cases, excluding the fit of Chi–MET data to Freundlich model.

Correlation coefficient values suggest that the Langmuir model provides a better fit to experimental adsorption data, compared to Freundlich model. Also, theoretical values of maximum adsorption capacity found for Langmuir isotherm is in good agreement with those obtained experimentally (Table 1). This result indicates that the adsorption on the bead surface probably occurred in monolayer fashion, as proposed by the Langmuir model, and only the amino groups are being part of the chelation of Cu(II). Results from Langmuir model also shows a decrease in parameter b, which means that although amino acid functionalized chitosan has increased its adsorption capacity, its interaction force with copper decreases.

A significant characteristic of Langmuir isotherm is the separation factor, R_L, a specific dimensionless constant defined as follows [33]:

$$R_L = \frac{1}{1 + bC_{ref}} \tag{5}$$

here b is the Langmuir constant related to the enthalpy of adsorption through the Van't Hoff equation, and C_{ref} is the initial concentration of adsorbate. R_L is used to predict the favorability of adsorption process, meaning unfavorable for $R_L > 1$, linear for $R_L = 1$, favorable for $0 < R_L < 1$, and irreversible $R_L = 0$.

R_L values for both natural and amino acid conjugated chitosan beads present favorable adsorption processes (Fig. 2). At lower concentrations, the values of R_L are close to 1, meaning the adsorption is less favorable compared to high concentration conditions, in which the values are close to 0. In the latter conditions, the adsorption process is extremely favorable, tending to irreversibility. These findings also agree with those obtained by fitting the adsorption data to the Freundlich model and analyzing the values of the adsorption intensity parameter, n. In all cases, we obtained n higher than 1.0 (Table 1), which also suggests that the adsorption
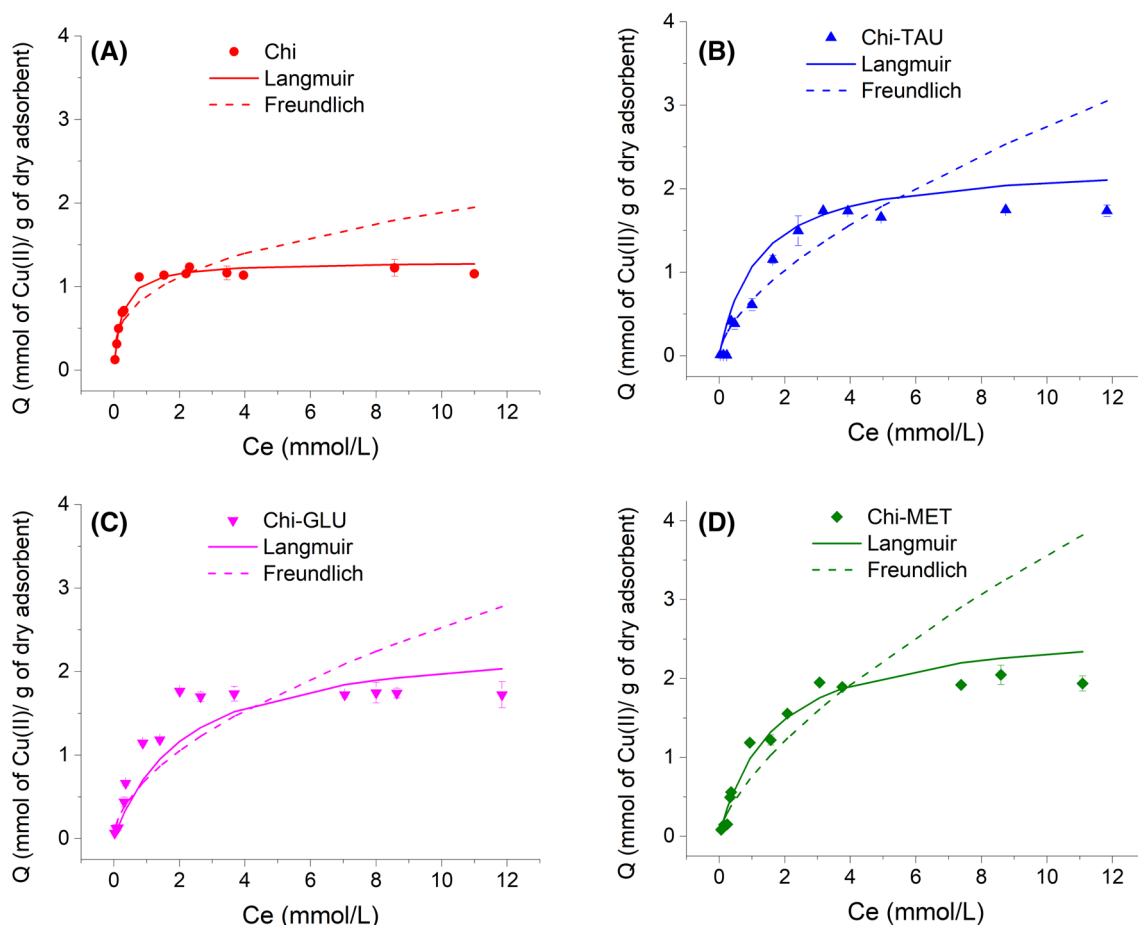
Fig. 1 Adsorption isotherms for Cu(II) on **a** natural chitosan beads (Chi) and chitosan beads functionalized with **b** taurine (Chi–TAU), **c** glutamic acid (Chi–GLU) and **d** methionine (Chi–MET) at pH 5.0 and 298 K. Symbols correspond to experimental data, solid line corresponds to Langmuir model and dashed line corresponds to Freundlich model

Table 1 Parameters of model-fitting to the experimental Cu(II) adsorption data at pH 5.0 and 298 K

	Langmuir model			Freundlich model		
	Q_{max} (mmol g^{-1})	b (L mmol^{-1})	R^2	K_f (mmol$^{1-1/n}$ L$^{1/n}$)/g	n	R^2
Chi	1.30 ± 0.04	4.02 ± 0.26	0.9852	0.89 ± 0.05	3.06 ± 0.34	0.8316
Chi–TAU	2.31 ± 0.17	0.86 ± 0.08	0.9660	0.67 ± 0.06	1.63 ± 0.10	0.8101
Chi–GLU	2.40 ± 0.10	0.57 ± 0.03	0.9853	0.72 ± 0.02	1.83 ± 0.08	0.9326
Chi–MET	2.68 ± 0.27	0.62 ± 0.09	0.9748	0.76 ± 0.08	1.49 ± 0.01	0.8297

Q_{max} experimental for Chi, Chi–TAU, Chi–GLU, and Chi–MET are, respectively, 1.17 mmol g^{-1}; 1.71 mmol g^{-1}; 1.73 mmol g^{-1} and 1.96 mmol g^{-1}

phenomenon is more favorable at higher Cu(II) concentration [34].

The three amino acid tested here led to a significative increase in maximum adsorption capacity of chitosan beads after conjugation step (Fig. 1). This may be primarily attributed to the new amide and hydroxyl chelating sites, and carboxylate groups, inserted in chitosan beads that contribute to Cu(II) uptake (see Fig. S1 in Supporting Information). The increase in adsorption capacity may also be associated with the increase in the spacing between chitosan chain after amino acid conjugation, enhancing the accessibility of Cu(II) to chelating sites of chitosan, which is ultimately related to the decrease in chitosan crystallinity, as suggested by other studies [35, 36]. Finally, the adsorption capacities reported here are substantially higher compared other modified chitosan-based adsorbents [28, 29, 37–39], although an accurate comparison to other
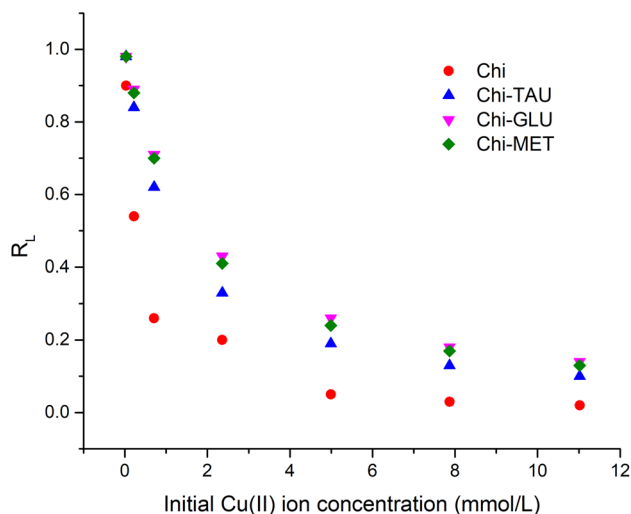
Fig. 2 Separation factor values, R_L, based on the Langmuir isotherm for Cu(II) adsorption on natural (Chi) and functionalized chitosan beads with taurine (Chi–TAU), glutamic acid (Chi–GLU) and methionine (Chi–MET) at pH 5.0 and 298 K

studies may be difficult due to lack of match between the experimental conditions employed.

Adsorption Kinetics

We tested three different kinetic models to investigate the rate controlling mechanism in the adsorption of Cu(II) in the amino acid functionalized chitosan beads, namely the pseudo-first-order, pseudo-second-order kinetic and the intraparticle diffusion models. The pseudo-first-order model, cited by Ho and McKay [40], was suggested by Lagergren [41] for the sorption of solid/liquid systems, and it has been used since then by many authors [28, 30, 42, 43], based on the following non-linear equation [29]:

$$Q_t = Q_e(1 - e^{-k_1 t}) \tag{6}$$

In Eq. 6, Q_t is the mass of Cu(II) adsorbed (g) at time (t), Q_e is the amount of adsorbed metal (mmol g^{-1}) at equilibrium and k_1 is the pseudo-first-order adsorption rate constant (s^{-1}).

The adsorption kinetics may also be described by a pseudo-second order model, proposed by Ho et al. [44], based on the hypothesis the adsorption process follows a chemisorption of second order mechanism, is represented by Eq. 7:

$$Q_t = Q_e \frac{Q_e k_2 t}{1 + Q_e k_2 t} \tag{7}$$

where Q_e is the amount of adsorbed metal (mmol g^{-1}) at equilibrium and k_2 is the pseudo-second-order adsorption rate constant (g mmol^{-1} s^{-1}).

The intraparticle diffusion model, proposed by Weber and Morris [45], is described by Eq. 8:

$$Q_t = k_i t^{0.5} \tag{8}$$

k_i is the intraparticle diffusion rate constant (mmol g^{-1} min$^{-0.5}$).

Figures S5 and 3 shows the data for the Cu(II) adsorption kinetic experiments with natural and amino acid functionalized chitosan beads and their respective curves for these three models. Equilibrium constants and adsorption rate constants for the pseudo-first-order and pseudo-second-order models are listed in Table 2, while the adsorption rate constants for the intraparticle diffusion model are listed in Table 3. These parameters were all obtained by employing the least-square method using the Origin® software and are presented with their correspondent correlation coefficient values (R^2).

Adsorption kinetic results (Fig. S5) show a fast adsorption during the first 16 h with almost 90% Cu(II) uptake in all cases, after which equilibrium is slowly achieved. The slower rates observed at the end of the experiment suggests the formation of a monolayer of Cu (II) on the outer surface of chitosan beads throughout the time, followed by the diffusion onto the inner surface of the adsorbent due to continuous stirring maintained during the experiment [44]. Results for all adsorbents tested show a high degree of correlation for both pseudo-first-order and pseudo-second-order models (Fig. S5 and Table 2), indicating that both could be used to describe Cu(II) adsorption. Also, values of adsorption capacity calculated by pseudo-first order model are very close to experimental data, suggesting the adsorption process occurred through reversible interactions between Cu(II) and the adsorbent surface with mass diffusion acting as the rate-limiting step. This result is in agreement with the Langmuir parameter R_L that also indicates a reversible adsorption at low Cu(II) concentrations.

Adsorption kinetics are usually controlled by the following four steps: (i) bulk diffusion: Cu(II) transfer from the bulk solution to the boundary film at the sorbent surface, (ii) film diffusion: Cu(II) transport from the boundary film to the surface of the adsorbent; (iii) intraparticle diffusion: transfer of Cu(II) from the surface to the intraparticle active sites and (iv) chemical reaction: uptake of Cu(II) via chelating, ion-exchange or complexation. Here, as the stirring speed is 150 rpm, we can not neglect any of these four steps, as opposed to experiments under stirring speed as high as 400 rpm, in which both bulk and film diffusion steps become irrelevant [46].

From Fig. 3, we also observe two inflection for both the natural and amino acid functionalized chitosan beads, which suggests the Cu(II) adsorption process is mediated by three different mechanisms in all cases. Here, the first portion may be attributed to the diffusion of Cu(II) into the film around
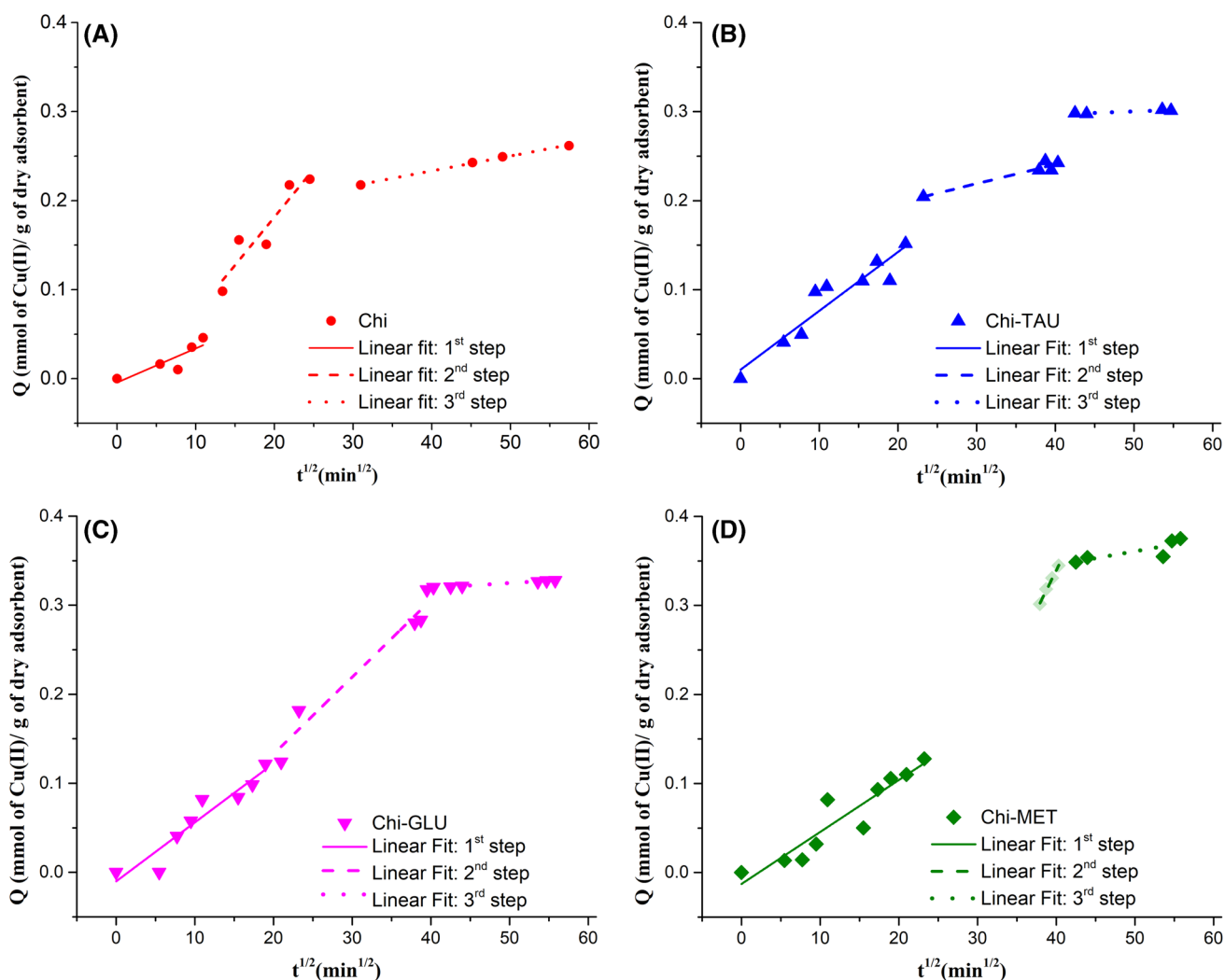
Fig. 3 Intraparticle diffusion model fits for kinetic uptake of Cu(II) using **a** natural (Chi) and functionalized chitosan beads with **b** taurine (Chi–TAU), **c** glutamic acid (Chi–GLU) and **d** methionine (Chi–MET) at pH 5.0 and 298 K. Experiments performed with an initial Cu(II) concentration of 0.480 mol L^{-1}

Table 2 Parameters and correlation coefficients for the pseudo-first-order and pseudo-second-order adsorption models for Cu(II) uptake using natural (Chi) and functionalized chitosan beads with taurine (Chi–TAU), glutamic acid (Chi–GLU) and methionine (Chi–MET) at pH 5.0 and 298 K

	Pseudo-first-order			Pseudo-second-order		
	Q_e (mmol g^{-1})	k_1 (s^{-1})	R^2	Q_e (mmol g^{-1})	k_2 (g mmol^{-1} s^{-1})	R^2
Chi	0.14 ± 0.01	0.04 ± 0.01	0.9734	0.22 ± 0.03	0.15 ± 0.05	0.9666
Chi–TAU	0.22 ± 0.04	0.11 ± 0.01	0.9916	0.28 ± 0.01	0.36 ± 0.05	0.9836
Chi–GLU	0.27 ± 0.01	0.13 ± 0.02	0.9073	0.32 ± 0.03	0.44 ± 0.10	0.9474
Chi–MET	0.39 ± 0.02	0.06 ± 0.01	0.9787	0.53 ± 0.04	0.09 ± 0.03	0.9661

the sorbent surface, while the second portion describes the continuous adsorption, and the third one is attributed to the final equilibrium stage or intraparticle diffusion. According to Findon et al. [47], the chemical reaction is a rapid step and may be neglected in these processes as well. From these three rate-limiting steps, we notice the lower slope

Table 3 Rate constants and correlation coefficients for the intraparticle diffusion model for Cu(II) uptake using natural (Chi) and functionalized chitosan beads with taurine (Chi–TAU), glutamic acid (Chi–GLU) and methionine (Chi–MET) at pH 5.0 and 298 K

| | Intraparticle diffusion | | | | | |
	$k_{i,1}$ (mmol g^{-1} $min^{-0.5}$)	R^2	$k_{i,2}$ (mmol g^{-1} $min^{-0.5}$)	R^2	$k_{i,3}$ (mmol g^{-1} $min^{-0.5}$)	R^2
Chi	0.23	0.6863	0.66	0.8354	0.10	0.9967
Chi–TAU	0.40	0.8753	1.26	0.8961	0.02	0.8218
Chi–GLU	0.40	0.8883	0.52	0.9392	0.03	0.9877
Chi–MET	0.35	0.8594	1.08	0.9974	0.10	0.5640

corresponds to the third portion of all curves (Table 3), indicating that the intraparticle diffusion of Cu(II) was the rate-limiting step for all the adsorbents studied here [48].

Characterization

SEM

Micrographies of natural and functionalized chitosan beads (Fig. 4) show that addition of amino acids into chitosan matrix led to the formation of large pore structures onto the surface of the adsorbents. Beppu et al. [49] examined the effect of porosity in chitosan membranes functionalized with histidine and indicated that membranes with higher porosity showed increased capacities of Cu(II) adsorption.

Deacetylation Degree (DD)

Potentiometric titration curves and the respective first derivatives were employed to calculate the deacetylation degree of natural and amino acid functionalized chitosan (Fig. 5). Based on Eq. 2, values of 60%, 86%, 97%, and 84% of DD we found to Chi, Chi–GLU, Chi–TAU, and Chi–MET, respectively, indicating an increase in the number of amino groups available due to the conjugation of chitosan with amino acids. Piron and Domard [50] assessed the influence of DD in adsorption capacity of uranyl ions in chitosan samples with different DD and they found that the adsorption capacity improved by increasing the DD. This is in good agreement with our findings, which also showed higher adsorption capacities for samples with higher DD, i.e., functionalized with amino acids (Table 1).

Fig. 4 SEM micrographs of natural (Chi) and amino acid functionalized chitosan beads (Chi–GLU, Chi–MET, and Chi–TAU)
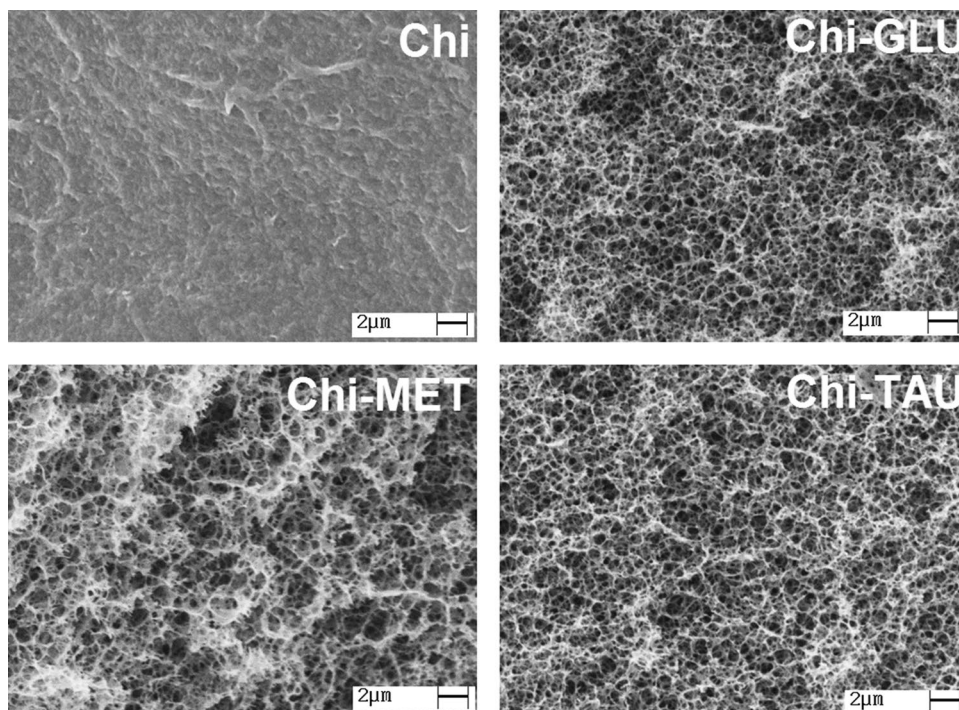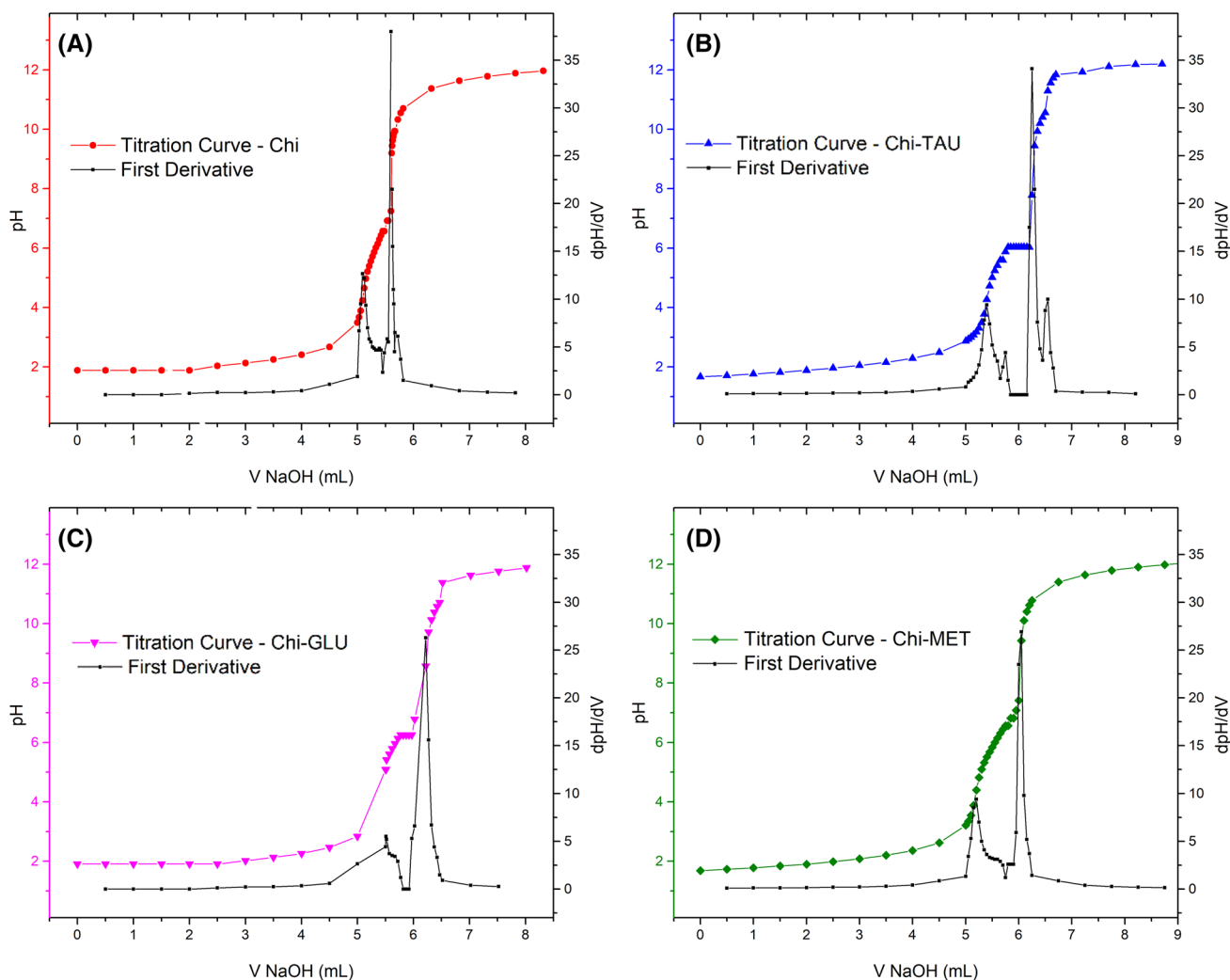
Fig. 5 Titration curves and the respective first derivatives of **a** natural (Chi) and functionalized chitosan beads with **b** taurine (Chi–TAU), **c** glutamic acid (Chi–GLU) and **d** methionine (Chi–MET)

FTIR-ATR and XPS

The IR spectra of natural and amino acid functionalized chitosan beads (Fig. 6) show similar features at around 3400 cm^{-1} (O–H stretching and N–H stretching), 2900 cm^{-1} (C–H stretching), 1650 cm^{-1} (C=O in the amide I), and 1560 cm^{-1} (NH-bending vibration in amide). Also, bands at 1418 and 1375 cm^{-1} could be assigned to CH and CH$_2$ vibrations respectively, 1070 and 1030 cm^{-1} (C–O–C stretching). The main changes observed in IR spectra after amino acid functionalization are observed at 1560 cm^{-1}, related to amide II of chitosan, that shifts to 1590 cm^{-1}. This change suggests the occurrence of new bonds that after functionalization or even an insertion of amino groups in chitosan matrix [51, 52]. Changes in the 3100–3500 cm^{-1} region suggest a partial contribution of hydroxyl groups in this functionalization reaction and the possible introduction of new amine and hydroxyl groups in chitosan. The C–S (around 700 cm^{-1}) [53] and =SO$_2$ (between 1000 and 1100 cm^{-1}) [54] bands that should appear for methionine and taurine is not detected, probably because of the weak signal that could be masked by the other vibrations founded in chitosan.

After Cu(II) adsorption, it is possible to notice the same modifications in all the IR spectra of amino acid functionalized beads, which implies that the adsorption process occurs through the same mechanisms in all the three adsorbents. After Cu(II) adsorption, the band at 3400 cm^{-1} (–OH and –NH), became broader, and the peak at 1590 cm^{-1} (–NH$_2$) disappeared, showing that the interaction with copper occurs with hydroxyl and amino groups which belong to both chitosan and amino acids inserted into the matrix.

By analyzing the C1s high-resolution spectra by XPS analysis (Fig. 7) it was possible to assert that the
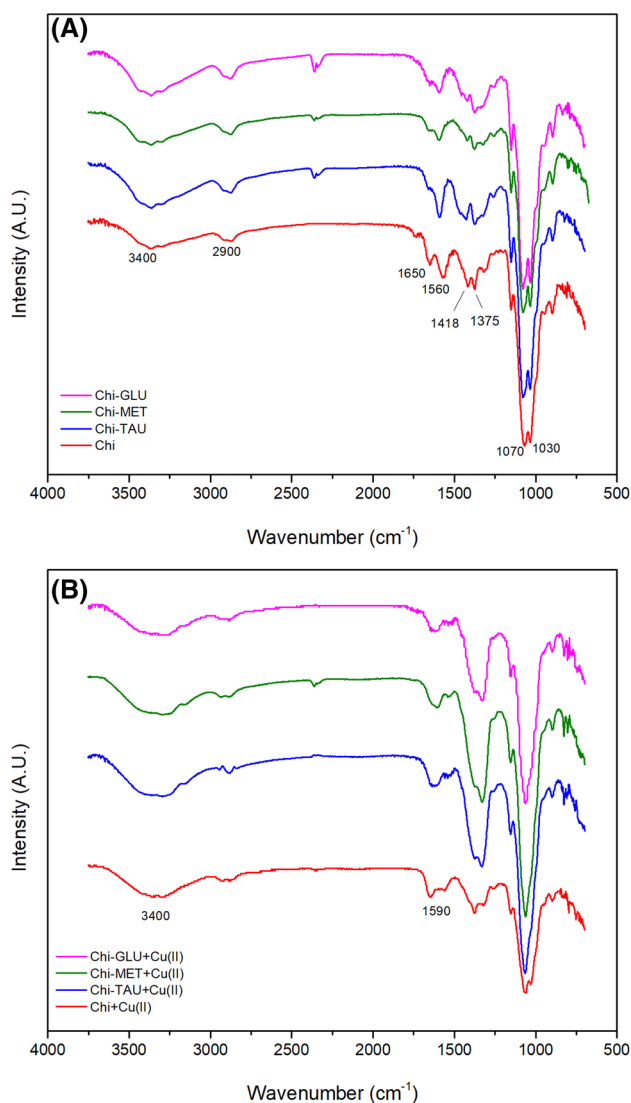
Fig. 6 IR spectra of natural (Chi) and functionalized chitosan beads with amino acids methionine (Chi–MET), glutamic acid (Chi–GLU) and taurine (Chi–TAU) **a** before and **b** after Cu(II) adsorption

Fig. 7 High-resolution spectra of carbon (C1s) for natural and amino acid functionalized chitosan beads

functionalization was achieved, since natural chitosan (Chi), complexed at pH 7, exhibited a large number of C–C bounds on its surface, while the functionalized beads presented a higher proportion of C–N, C–O, and O–C–O bounds. This result indicates that more functional groups, derived from the amino acids, were inserted on the bead surfaces, which agrees with the FTIR data. In addition, the C1s spectra are very similar to the functionalized beads, regardless of the amino acid used. A possible hypothesis is that even though the amino acids differ from each other in their side-chain structures, the functional groups exposed on the bead surface may be the same. This may also explain why the Cu(II) adsorption results were very similar to these functionalized samples.
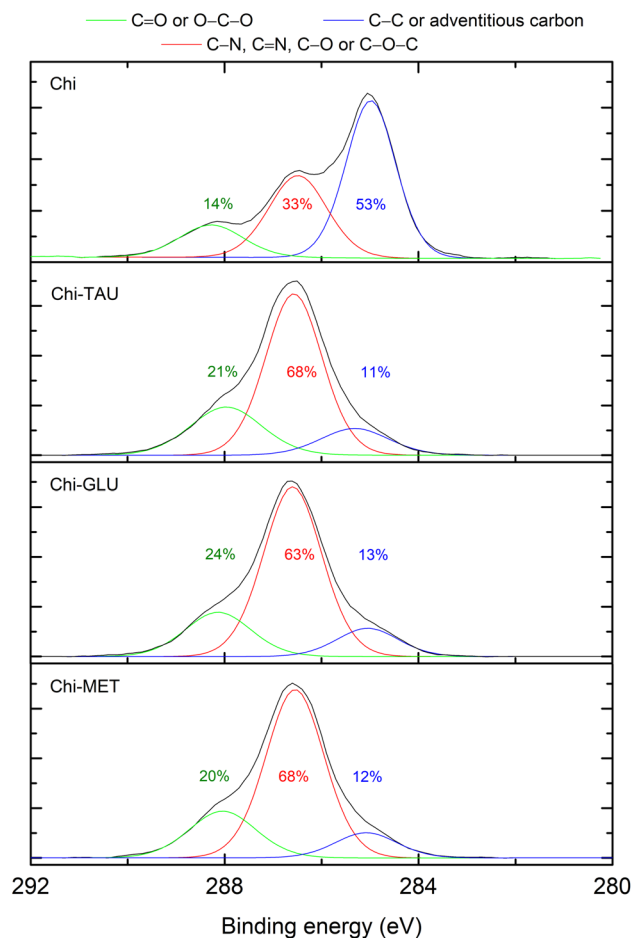
We also verified for the N1s high-resolution spectra acquired by XPS that the peak area related to the group $-NH_3^+$ presented a larger area for natural chitosan beads compared to the modified beads after the copper uptake (Fig. 8). This result indicates that the formation of the complex $R-NH_2Cu^{2+}$ is more favorable for the original beads and its higher bind energy value may justify why copper binds stronger to natural chitosan beads than to the functionalized ones. For the formation of this complex, a nitrogen atom shares a pair of electrons with Cu(II), the reason why the electronic density of nitrogen atoms is reduced. Thus, a higher energy is required for the removal of electrons during the XPS analysis, resulting in higher values of binding energy to N1s peak. Consequently, the larger the area relative to the NH_3^+ peak, the stronger the interaction between the nitrogen-containing functional groups and the copper, which is in good agreement with the b, R_L an n parameters from the Langmuir and Freundlich models, respectively.
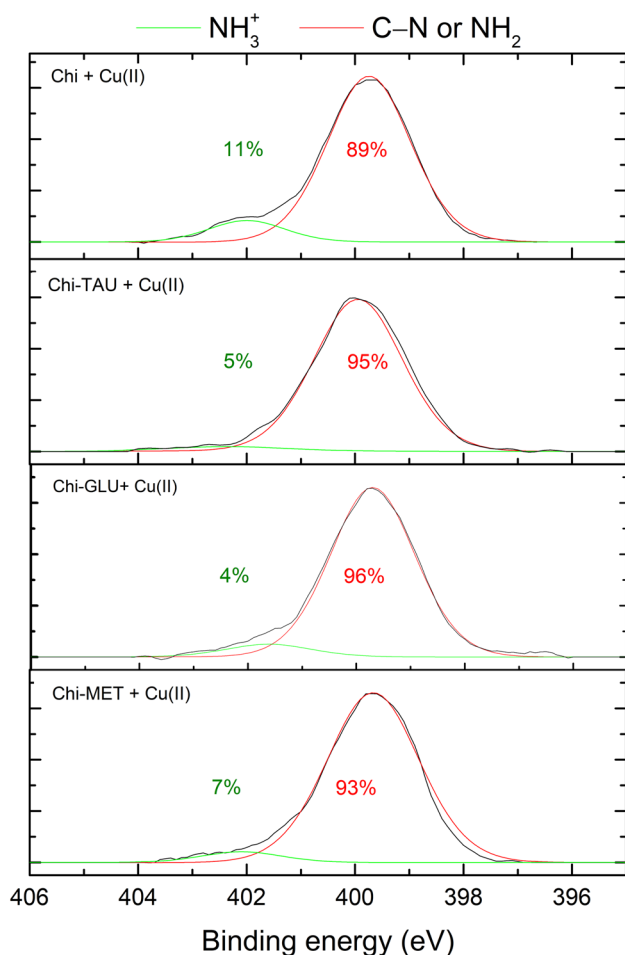
Fig. 8 High-resolution spectra of nitrogen N1s for pristine and functionalized chitosan beads after Cu(II) uptake

Conclusion

In summary, this study indicates amino acids functionalization of chitosan beads improves their Cu(II) adsorption capacity, possibly due to the addition of new chelating and electrostatic sites in the polymer matrix. Isotherm experiments provided a good fit for the Langmuir model, showing an increase in maximum adsorption capacity for Cu(II) from 1.30 mmol g^{-1} prior to amino acid conjugation to values as high as 2.31 mmol g^{-1}, 2.40 mmol g^{-1} and 2.68 mmol g^{-1} for Chi–TAU, Chi–GLU, and Chi–MET, respectively. Also, kinetic adsorption experiments indicated a better fit for the pseudo-first-order model, while intraparticle diffusion model suggested a three-step mechanism for Cu(II) uptake, limited by the third, intraparticle diffusion, step. Amino acid functionalized chitosan beads present great potential as adsorbents treatment of wastewater effluents contaminated Cu(II). Besides, after Cu(II) adsorption, these materials may be further explored in applications that demand metal ion interactions, such as their use as supports for proteins with high affinity for metal ion for protein purification purposes.

Compliance with Ethical Standards

Conflict of interest The authors have no conflict of interest to declare.

References

1. Fu F, Wang Q (2011) Removal of heavy metal ions from wastewaters: a review. J Environ Manag 92(3):407–418
2. Li J, Tong J, Li X, Yang Z, Zhang Y, Diao G (2016) Facile microfluidic synthesis of copolymer hydrogel beads for the removal of heavy metal ions. J Mater Sci 51(23):10375–10385
3. USEPA (United Station Environmental Protection Agency) (2010) Lead and copper rule monitoring and reporting guidance for public water systems (EPA-816-R-02-009). Ground Water and Drinking Water Division, Water Programs, Washington, DC
4. Chen Q, Luo Z, Hills C, Xue G, Tyrer M (2009) Precipitation of heavy metals from wastewater using simulated flue gas: sequent additions of fly ash, lime and carbon dioxide. Water Res 43(10):2605–2614
5. Samper E, Rodríguez M, De la Rubia M, Prats D (2009) Removal of metal ions at low concentration by micellar-enhanced ultrafiltration (MEUF) using sodium dodecyl sulfate (SDS) and linear alkylbenzene sulfonate (LAS). Sep Purif Technol 65(3):337–342
6. Khelifa A, Moulay S, Naceur A (2005) Treatment of metal finishing effluents by the electroflotation technique. Desalination 181(1–3):27–33
7. Chang Q, Wang G (2007) Study on the macromolecular coagulant PEX which traps heavy metals. Chem Eng Sci 62(17):4636–4643
8. Rabelo R, Vieira R, Luna F, Guibal E, Beppu M (2012) Adsorption of copper (II) and mercury (II) ions onto chemically-modified chitosan membranes: equilibrium and kinetic properties. Adsorpt Sci Technol 30(1):1–21
9. Yu Y, Peng R, Yang C, Tang Y (2015) Eco-friendly and cost-effective superabsorbent sodium polyacrylate composites for environmental remediation. J Mater Sci 50(17):5799–5808
10. Albarelli JQ, Rabelo RB, Santos DT, Beppu MM, Meireles MAA (2011) Effects of supercritical carbon dioxide on waste banana peels for heavy metal removal. J Supercrit Fluids 58(3):343–351
11. Oliveira LS, Franca AS, Alves TM, Rocha SD (2008) Evaluation of untreated coffee husks as potential biosorbents for treatment of dye contaminated waters. J Hazard Mater 155(3):507–512
12. Rinaudo M (2006) Chitin and chitosan: properties and applications. Prog Polym Sci 31(7):603–632
13. Deans JR, Dixon BG (1992) Uptake of Pb2 + and Cu2 + by novel biopolymers. Water Res 26(4):469–472
14. Vieira RS, Lisa M, Oliveira M, Guibal E, Rodríguez-castellón E, Beppu MM (2011) Copper, mercury and chromium adsorption on natural and crosslinked chitosan films: an XPS investigation of mechanism. Colloids Surf A 374(1–3):108–114

15. Steenkamp G, Keizer K, Neomagus H, Krieg H (2002) Copper (II) removal from polluted water with alumina/chitosan composite membranes. J Membr Sci 197(1):147–156

16. Guibal E (2004) Interactions of metal ions with chitosan-based sorbents: a review. Sep Purif Technol 38(1):43–74

17. Beppu MM, Vieira RS, Aimoli CG, Santana CC (2007) Crosslinking of chitosan membranes using glutaraldehyde: effect on ion permeability and water absorption. J Membr Sci 301(1–2):126–130

18. Fu H, Kobayashi T (2010) Self-assembly functionalized membranes with chitosan microsphere/polyacrylic acid layers and its application for metal ion removal. J Mater Sci 45(24):6694–6700

19. Boggione MaJ, Mahl CRA, Beppu MM, Farruggia B (2017) Synthesis and characterization of chitosan membranes functionalized with amino acids and copper for adsorption of endoglucanase. Powder Technol 315:250–257

20. Demir AG, Taketa TB, Tolouei R, Furlan V, Paternoster C, Beppu MM, Mantovani D, Previtali B (2015) Laser surface structuring affects polymer deposition, coating homogeneity, and degradation rate of Mg alloys. Mater Lett 160:359–362

21. Vasconcellos FC, Goulart GAS, Beppu MM (2011) Production and characterization of chitosan microparticles containing papain for controlled release applications. Powder Technol 205(1–3):65–70

22. Vieira RS, Beppu MM (2005) Mercury ion recovery using natural and crosslinked chitosan membranes. Adsorption 11:731–736

23. Oshita K, Sabarudin A, Takayanagi T, Oshima M, Motomizu S (2009) Adsorption behavior of uranium (VI) and other ionic species on cross-linked chitosan resins modified with chelating moieties. Talanta 79(4):1031–1035

24. Inoue K, Yoshizuka K, Ohto K (1999) Adsorptive separation of some metal ions by complexing agent types of chemically modified chitosan. Anal Chim Acta 388(1):209–218

25. Casettari L, Vllasaliu D, Lam JKW, Soliman M, Illum L (2012) Biomedical applications of amino acid-modi fi ed chitosans: a review. Biomaterials 33(30):7565–7583

26. Sano T, Murase I (1980) US Patent 4,200,735. U.S. Patent and Trademark Office, Washington, DC

27. Adhikari CR, Parajuli D, Inoue K, Ohto K, Kawakita H (2008) Pre-concentration and separation of heavy metal ions by chemically modified waste paper gel. Chemosphere 72(2):182–188

28. Li N, Bai R (2005) Copper adsorption on chitosan-cellulose hydrogel beads: behaviors and mechanisms. Sep Purif Technol 42(3):237–247

29. Ngah WSW, Fatinathan S (2008) Adsorption of Cu(II) ions in aqueous solution using chitosan beads, chitosan-GLA beads and chitosan-alginate beads. Chem Eng J 143(1–3):62–72

30. Zhao F, Yu B, Yue Z, Wang T, Wen X, Liu Z, Zhao C (2007) Preparation of porous chitosan gel beads for copper(II) ion adsorption. J Hazard Mater 147(1–2):67–73

31. Langmuir I (1918) The adsorption of gases on plane surfaces of glass, mica and platinum. J Am Chem Soc 40(9):1361–1403

32. Freundlich H (1907) Über die adsorption in lösungen. Z Phys Chem 57:385–470

33. Hall KR, Eagleton LC, Acrivos A, Vermeulen T (1966) Pore- and solid-diffusion kinetics in fixed-bed adsorption under constant-pattern conditions. Ind Eng Chem Fundam 5(2):212–223

34. Al-Degs YS, El-Barghouthi MI, Issa AA, Khraisheh MA, Walker GM (2006) Sorption of Zn(II), Pb(II), and Co(II) using natural sorbents: equilibrium and kinetic studies. Water Res 40(14):2645–2658

35. Monteiro OA, Airoldi C (1999) Some studies of crosslinking chitosan–glutaraldehyde interaction in a homogeneous system. Int J Biol Macromol 26(2):119–128

36. Kurita K, Koyama Y, Taniguchi A (1986) Studies on chitin. IX. Crosslinking of water-soluble chitin and evaluation of the products as adsorbents for cupric ion. J Appl Polym Sci 31(5):1169–1176

37. Wan Ngah WS, Endud CS, Mayanar R (2002) Removal of copper(II) ions from aqueous solution onto chitosan and crosslinked chitosan beads. React Funct Polym 50(2):181–190

38. Wan Ngah WS, Kamari A, Koay YJ (2004) Equilibrium and kinetics studies of adsorption of copper (II) on chitosan and chitosan/PVA beads. Int J Biol Macromol 34(3):155–161

39. Wan Ngah WS, Teong LC, Hanafiah MAKM (2011) Adsorption of dyes and heavy metal ions by chitosan composites: a review. Carbohydr Polym 83(4):1446–1456

40. Ho Y-S, McKay G (2000) The kinetics of sorption of divalent metal ions onto sphagnum moss peat. Water Res 34(3):735–742

41. Lagergren SY (1898) Zur Theorie der sogenannten adsorption gelöster stoffe. Handlingar, Stockholm

42. Baroni P, Vieira RS, Meneghetti E, da Silva MGC, Beppu MM (2008) Evaluation of batch adsorption of chromium ions on natural and crosslinked chitosan membranes. J Hazard Mater 152(3):1155–1163

43. Papageorgiou SK, Kouvelos EP, Katsaros FK (2008) Calcium alginate beads from Laminaria digitata for the removal of Cu + 2 and Cd + 2 from dilute aqueous metal solutions. Desalination 224(1–3):293–306

44. Ho YS, Wase DAJ, Forster CF (1995) Batch nickel removal from aqueous solution by sphagnum moss peat. Water Res 29(5):1327–1332

45. Weber WJ, Morris JC (1963) Kinetics of adsorption on carbon from solution. J Sanitary Eng Div 89:31–60

46. Lee ST, Mi FL, Shen YJ, Shyu SS (2001) Equilibrium and kinetic studies of copper(II) ion uptake by chitosan-tripolyphosphate chelating resin. Polymer 42(5):1879–1892

47. Findon A, McKay G, Blair HS (1993) Transport studies for the sorption of copper ions by chitosan. J Environ Sci Health A 28:173–185

48. Popuri SR, Vijaya Y, Boddu VM, Abburi K (2009) Adsorptive removal of copper and nickel ions from water using chitosan coated PVC beads. Bioresour Technol 100(1):194–199

49. Beppu M, Arruda E, Vieira R, Santos N (2004) Adsorption of Cu (II) on porous chitosan membranes functionalized with histidine. J Membr Sci 240(1):227–235

50. Piron E, Domard A (1997) Interaction between chitosan and uranyl ions. Part 1. Role of physicochemical parameters. Int J Biol Macromol 21(4):327–335

51. Pawlak A, Mucha M (2003) Thermogravimetric and FTIR studies of chitosan blends. Thermochim Acta 396(1–2):153–166

52. Ritthidej GC, Phaechamud T, Koizumi T (2002) Moist heat treatment on physicochemical change of chitosan salt films. Int J Pharm 232(1–2):11–22

53. Mary MB, Umadevi M, Pandiarajan S, Ramakrishnan V (2004) Vibrational spectral studies of l-methionine l-methioninium perchlorate monohydrate. Spectrochim Acta A 60(11):2643–2651

54. Triebel S, Sproll C, Reusch H, Godelmann R, Lachenmeier DW (2007) Rapid analysis of taurine in energy drinks using amino acid analyzer and Fourier transform infrared (FTIR) spectroscopy as basis for toxicological evaluation. Amino Acids 33(3):451–457